


Characterization of an experimental model to determine streptococcal M protein–induced autoimmune cardiac and neurobehavioral abnormalities

Rukshan AM Rafeek¹ , Adam S Hamlin¹, Nicholas M Andronicos¹, Craig S Lawlor¹, David J McMillan^{1,2}, Kadaba S Sriprakash^{1,3} & Natkunam Ketheesan^{1,2}

¹ School of Science & Technology, University of New England, Armidale, NSW, Australia

² School of Science, Technology, Engineering and Genecology Research Centre, University of the Sunshine Coast, Sippy Downs, QLD, Australia

³ Infection and Inflammation Laboratory, QIMR Berghofer Medical Research Institute, Herston, QLD, Australia

Keywords

Autoimmunity, group A streptococcus, Lewis rat model, rheumatic heart disease, *Streptococcus dysgalactiae* subspecies *equisimilis*, sydenham chorea

Correspondence

Rukshan AM Rafeek, School of Science & Technology, University of New England, McClymont Building (W34), Trevenna Rd, Armidale, NSW 2351, Australia.

E-mail: rmohame2@myune.edu.au

Received 6 April 2022;

Revised 28 June 2022;

Accepted 5 July 2022

doi: 10.1111/imcb.12571

Immunology & Cell Biology 2022; 100: 653–666

Abstract

Group A streptococcal (GAS) infection is associated with a spectrum of autoimmune diseases including acute rheumatic fever/rheumatic heart disease (ARF/RHD) and neurobehavioral abnormalities. Antibodies against GAS M proteins cross-react with host tissue proteins in the heart and brain leading to the symptomatology observed in ARF/RHD. As throat carriage of *Streptococcus dysgalactiae* subspecies *equisimilis* (SDSE) has been reported to be relatively high in some ARF/RHD endemic regions compared with GAS, and both SDSE and GAS express coiled-coil surface protein called M protein, we hypothesized that streptococci other than GAS can also associated with ARF/RHD and neurobehavioral abnormalities. Neurobehavioral assessments and electrocardiography were performed on Lewis rats before and after exposure to recombinant GAS and SDSE M proteins. Histological assessments were performed to confirm inflammatory changes in cardiac and neuronal tissues. ELISA and Western blot analysis were performed to determine the cross-reactivity of antibodies with host connective, cardiac and neuronal tissue proteins. Lewis rats injected with M proteins either from GAS or SDSE developed significant cardiac functional and neurobehavioral abnormalities in comparison to control rats injected with phosphate-buffered saline. Antibodies against GAS and SDSE M proteins cross-reacted with cardiac, connective and neuronal proteins. Serum from rats injected with streptococcal antigens showed higher immunoglobulin G binding to the striatum and cortex of the brain. Cardiac and neurobehavioral abnormalities observed in our experimental model were comparable to the cardinal symptoms observed in patients with ARF/RHD. Here for the first time, we demonstrate in an experimental model that M proteins from different streptococcal species could initiate and drive the autoimmune-mediated cardiac tissue damage and neurobehavioral abnormalities.

INTRODUCTION

Group A streptococcal (GAS) infection triggers autoimmune sequelae, which include acute rheumatic fever (ARF) and rheumatic heart disease (RHD).¹ Sydenham chorea (SC), an immune-mediated

neurobehavioral complication, is observed in approximately 30% of patients with ARF resulting in movement and behavioral abnormalities.¹ The pathogenesis of ARF/RHD and associated neurobehavioral disorders is complex and multifaceted. In general, an autoimmune response triggered by GAS

infection elicits antibodies that react with specific pathogen molecules and selected host proteins, leading to cardiac tissue damage and neurobehavioral abnormalities.² Various host proteins including cardiac and connective tissue proteins such as cardiac myosin,³ tropomyosin,⁴ laminin,⁵ keratin,⁶ vimentin⁶ and collagen^{7–9} are associated with this autoimmune process that leads to ARF/RHD.¹

Our current understanding of the immune mechanisms leading to SC remains rudimentary. However, antigenic similarity between GAS proteins and neuronal proteins such as dopamine receptors 1 and 2 (DR1 and DR2), lysoganglioside and tubulin is hypothesized to be responsible for the abnormalities associated with SC. In SC, cross-reactive neuron-specific antibodies target basal ganglia, and this might be due to the presence of dopaminergic neurons in the striatum which share antigenic similarity to GAS antigens.¹⁰ The mechanisms that compromise the blood–brain barrier and facilitate the migration of these cross-reactive antibodies that bind to neuronal tissue remain under investigation. In addition, heterogeneity of the immune response against the immunodominant epitopes of GAS M protein and group A carbohydrate epitope *N*-acetyl- β -D-glucosamine may facilitate epitope spreading and cross-recognition of several host antigens leading to tissue injury.¹

Streptococcus dysgalactiae subspecies *equisimilis* (SDSE), also commonly known as group G streptococcus, has similar virulence genes and antigenic properties as those of GAS and exhibits an overlapping spectrum of disease presentations with GAS.^{11–16} Although a direct association between SDSE infection and ARF/RHD has not been widely reported, epidemiological studies from some ARF/RHD endemic areas show that pharyngeal carriage of GAS is relatively low compared with SDSE.^{17,18} In 2018, the first case of a neuropsychiatric disorder similar to SC associated with SDSE infections was reported in Japan.¹⁹ Given the similar virulence profiles and tissue tropism of GAS and SDSE,²⁰ it is plausible that SDSE may cause or exacerbate ARF/RHD. Indeed, our earlier experimental studies showed that SDSE could also cause and exacerbate cardiac impairment similar to ARF/RHD in the Lewis rat autoimmune valvulitis (RAV) model.²¹ Recent studies using this same model have shown the simultaneous induction of both cardiac and neurobehavioral abnormalities in Lewis rats following exposure to GAS antigens.²² These observations reinforce the importance of understanding the role of both GAS and SDSE in the pathogenesis of ARF/RHD and SC. Moreover, lack of a suitable animal model hindered the progress of understanding the pathogenesis of ARF/RHD and associated neurobehavioral changes, development of vaccines against GAS infections and

identification of disease-associated biomarkers for the diagnosis of ARF/RHD.²³ Therefore, it is hypothesized that GAS and SDSE M proteins could induce cross-reactive antibodies in the RAV model, leading to both carditis and neurobehavioral complications akin to the symptomatology observed in ARF/RHD. To test this hypothesis, we utilized the M protein gene (*stg480*) from an SDSE clinical isolate (NS3396) from a patient with a definitive diagnosis of ARF from the Northern Territory of Australia.²⁰ In this study, the functional and histological changes observed in the heart, and neurobehavioral and immunohistochemical changes in brains of Lewis rats injected with recombinant M proteins of GAS M5 (GAS rM5) and SDSE (SDSE Stg480) are reported.

RESULTS

Antibodies against streptococcal recombinant proteins recognize host tissue proteins

We first analyzed sera from rats injected with streptococcal recombinant proteins or phosphate-buffered saline (PBS) to determine the immunoglobulin G (IgG) response by ELISA. All rats injected with GAS rM5 and SDSE Stg480 had significantly higher ($P < 0.01$) IgG reactivity to GAS rM5 and SDSE Stg480 protein, respectively, than sera from PBS-injected control rats. We also determined the cross-reactivity of these antibodies with host tissue protein. Immune sera from rats injected with GAS rM5 and SDSE Stg480 showed significantly higher titer of antibody reactivity against cardiac myosin, tropomyosin, laminin, collagens I and IV (denatured), DR1 and DR2, tubulin and lysoganglioside_{GMI} ($P < 0.01$) than the titer of sera from PBS-injected control rats (Figure 1; [Supplementary figure 1](#)). Therefore, immune sera from rats challenged with streptococcal recombinant proteins cross-reacted with cardiac, connective and neuronal proteins. Cross-reactivity of antibodies against streptococcal antigens with host tissue proteins is a hallmark of ARF/RHD, wherein these polyclonal antibodies bind proteins present in host tissue.

Exposure to streptococcal recombinant proteins induce conduction abnormalities and inflammatory changes in heart tissue

Electrocardiography (ECG) was performed to assess the conduction abnormalities in rats injected with GAS rM5 or SDSE Stg480 antigens. Significant prolongation of P–R intervals was observed in all the rats injected with GAS rM5 ($P = 0.0007$) and SDSE Stg480 ($P = 0.0036$)

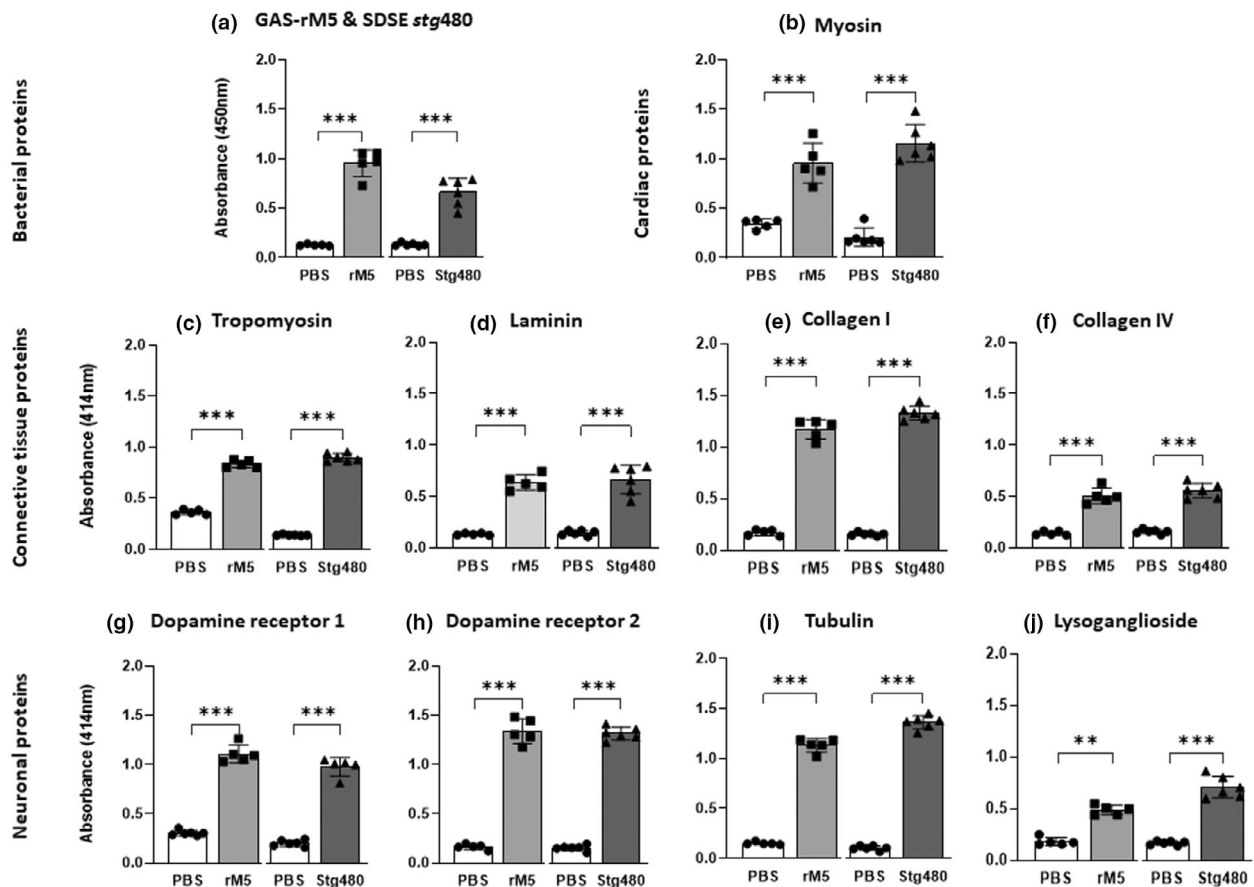


Figure 1. Antibodies generated following exposure to streptococcal recombinant proteins react with different host proteins. Indirect ELISAs were performed in duplicates to determine host protein cross-reactivity of rat sera from GAS rM5 (closed squares), SDSE Stg480 antigen-injected rats (closed triangles) and PBS controls (closed circles). Significantly ($P < 0.01$) higher titers of (a) serum IgG reactivity were observed in rats injected with GAS rM5 and SDSE Stg480 with corresponding antigens and cross-reactivity against host proteins including (b) cardiac myosin, (c) tropomyosin, (d) laminin, collagens (e) I and (f) IV, (g) DR1 and (h) DR2, (i) tubulin and (j) lysoganglioside_{GM1} than in control rats injected with PBS. Data are from one of two experiments with age-matched rats injected with GAS rM5 ($n = 5$) and SDSE Stg480 ($n = 6$). Error bars represent standard errors of the mean. ** $P < 0.01$, *** $P < 0.001$, by one-way ANOVA with Tukey's *post hoc* multiple comparison test. DR, dopamine receptor; GAS, group A streptococcus; Ig, immunoglobulin; PBS, phosphate-buffered saline; SDSE, *Streptococcus dysgalactiae* subspecies *equisimilis*.

compared with PBS-injected control rats (Figure 2a). Prolonged P–R interval is a minor Jones criterion in the diagnosis of ARF/RHD.

Hematoxylin and eosin staining of *post mortem* cardiac tissue from streptococcal antigen-injected rats suggested an inflammatory response in this tissue. Specifically, heart tissues from rats injected with GAS rM5 and SDSE Stg480 demonstrated evidence of carditis and valvulitis with infiltration of mononuclear cells (Figure 2d, e, g, h). Little or no evidence of infiltration of mononuclear leukocytes was observed in the myocardium and valves of the control rats that were injected with PBS. Carditis scores were determined based on the number of mononuclear cell infiltration

in both mitral valve and myocardium from rats injected with GAS rM5 ($n = 5$) SDSE Stg480 ($n = 6$) and PBS ($n = 6$). Carditis scores (Figure 2b) were significantly higher ($P < 0.001$) in Lewis rats injected with GAS-rM5 and SDSE Stg480 than in control rats injected with PBS.

Immunohistochemical analysis was performed to determine the type of mononuclear cells infiltrating the cardiac tissue. From formalin-fixed, paraffin-embedded sections (Figure 3), T cells were detected using an antibody against the pan T-cell marker CD3, whereas macrophages were detected by CD68 marker expression. Mononuclear cells in valvular and myocardial lesions were mainly CD3⁺ T lymphocytes and CD68⁺

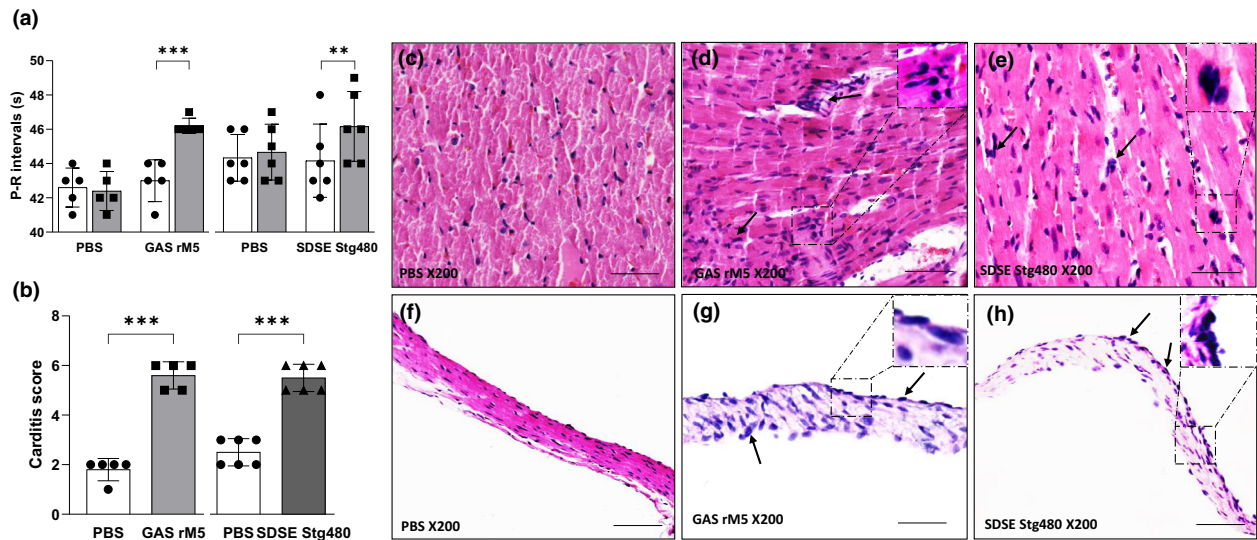


Figure 2. Electrocardiographic and histological changes demonstrate functional impairment and inflammatory changes in the cardiac tissue of rats exposed to streptococcal recombinant proteins. **(a)** Prolongation of P–R intervals was observed in rats injected with streptococcal recombinant proteins compared with control rats. **(b)** Carditis scores were significantly higher in rats injected with GAS rM5 (closed squares) and SDSE Stg480 (closed triangles) than control rats (closed circles). Characteristic mononuclear cell infiltrations (arrows) were observed in the **(d, e)** myocardium and **(g, h)** valvular tissues of rats injected with GAS rM5 and SDSE Stg480 compared with **(c, f)** rats injected with PBS. Data are from one of two experiments with age-matched rats injected with GAS rM5 ($n = 5$) and SDSE Stg480 ($n = 6$). $**P < 0.01$, $***P < 0.001$, by one-way ANOVA and the Mann–Whitney U -test. Bars = 50 μm . GAS, group A streptococcus; PBS, phosphate-buffered saline; SDSE, *Streptococcus dysgalactiae* subspecies *equisimilis*.

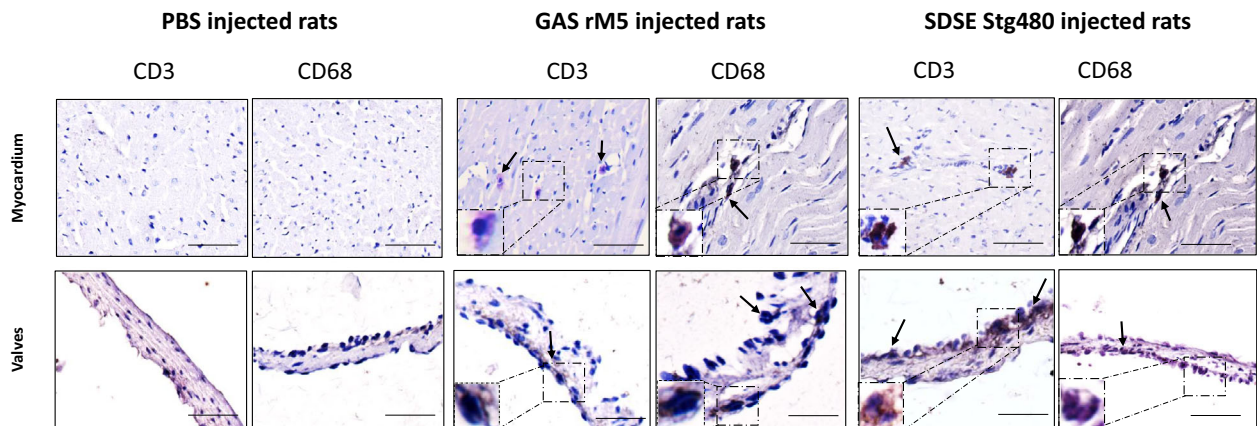


Figure 3. T cells and macrophages infiltrate into cardiac tissue of rats injected with streptococcal recombinant proteins. Rat hearts were stained using antibodies against CD3 to detect infiltrating T cells and CD68 to detect macrophages (arrows). Rats injected with GAS rM5 and SDSE M protein had significantly increased infiltration of CD3⁺ T cells and CD68⁺ macrophages. By contrast, control rats injected with PBS had no evidence of infiltration of CD3⁺ T cells or macrophages. Representative microscopic images of myocardium and valves from an age-matched rat injected with GAS rM5 and SDSE Stg480. Both CD3⁺ T cells and CD68⁺ macrophages were observed in all cardiac tissues collected from three individual age-matched rats injected with GAS rM5 ($n = 3$) and SDSE Stg480 ($n = 3$). Bars = 50 μm . GAS, group A streptococcus; PBS, phosphate-buffered saline; SDSE, *Streptococcus dysgalactiae* subspecies *equisimilis*.

macrophages, suggesting that these leukocytes were associated with inflammatory damage in rats injected with streptococcal antigens. No infiltration of CD3⁺ or CD68⁺ leukocytes was observed in the valves or myocardium in rats injected with PBS.

Neurobehavioral abnormalities in rats following exposure to streptococcal recombinant proteins

Pre (baseline) and post exposure behavioral responses of rats injected with streptococcal recombinant proteins

were compared with PBS-injected control rats to determine the motor and compulsive behavioral abnormalities. Standardized behavioral tests including food manipulation, beam walking, marble burying, grooming and light/dark box tests were performed on all rats (Figure 4). Significant impudence in manipulating food pellets when compared with control rats was observed in rats injected with GAS rM5 ($P = 0.0066$) and SDSE Stg480 ($P = 0.0107$). The abnormalities in gait and balance were assessed by a beam walking test. Rats injected with GAS rM5 ($P = 0.0066$) and SDSE Stg480 ($P = 0.0028$) took significantly more time in traversing the narrow (2.5 cm) beam. Significantly increased grooming was observed in rats injected with GAS rM5 ($P < 0.0001$) and SDSE Stg480 ($P < 0.0001$) compared with rats injected with PBS on all 3 days of observation. Rats injected with GAS rM5 ($P < 0.0001$) and SDSE Stg480 ($P = 0.0020$) buried significantly higher number of marbles than control rats, which suggested the repetitive and compulsive-like behaviors of rats injected with streptococcal antigens. However, no significant differences were observed between rats injected with streptococcal recombinant proteins and PBS-injected control rats in the time that rats spent in the light area ($P = 0.4909$), the number of entries to the light compartment ($P = 0.8523$) and latency to first entry to the light compartment ($P = 0.3723$) in the light/dark box test, thereby suggesting that none of the rats developed anxiety-like behavior (Supplementary figure 2).

Serum IgG binds to neuronal tissue

The pattern of *in vivo* IgG deposition on to neuronal membranes in the striatum of streptococcal antigen-injected rats and PBS control rats was indistinct. Therefore, to confirm the pattern of IgG binding on the striatum, exogenous antisera from streptococcal M protein-injected and PBS-injected rats was used to probe various regions of the brain *in vitro*. The exogenous serum from rats injected with streptococcal recombinant proteins showed significantly increased IgG binding to the striatum and cortex (Figure 5). By contrast, sections incubated with serum from rats injected with PBS and sections incubated with PBS showed a weak nonspecific IgG staining pattern on the striatum and cortex.

Immunoreactivity of serum IgG with endogenous and purified neuronal proteins

Qualitative western blots analysis (Figure 6; Supplementary figure 3) was performed to demonstrate the binding of antibodies in serum from streptococcal antigen-injected rats with host proteins. Western blots

were also performed to confirm cross-reactivity of serum IgG from rats injected with streptococcal recombinant proteins with purified DR1 and DR2, tubulin and lysoganglioside_{GM1}. The specificity of the cross-reactive anti-GAS and anti-SDSE antibody binding with endogenous host antigens in the striatum and cerebellum from brain tissue of naïve rats was also confirmed by western blot analysis. Serum from rats injected with streptococcal recombinant proteins were strongly immunoreactive to purified DR1 and DR2, tubulin and lysoganglioside_{GM1} (Figure 6a, b; Supplementary figure 3). No specific immunoreactivity was observed with purified neuronal proteins against sera from control rats injected with PBS. Moreover serum from rats injected with streptococcal recombinant proteins recognized endogenous striatum and cerebellum antigens in the nonreducing western blot (Figure 6c, d; Supplementary figure 3). Western blot analysis revealed that both sera from GAS rM5 and SDSE Stg480 recognized an immunodominant 55- and 70-kDa protein in the striatum and cerebellum but not in the non-neuronal control tissue (kidney). Thus, these immunoreactive proteins, detected by GAS rM5 and SDSE Stg480 immune sera, in the brain lysates may be from neurons in these striatum and cerebellum homogenates.

DISCUSSION

Historically, the etiology of ARF/RHD is attributed to preceding GAS infections.¹ Similar repeated findings by many investigators have hampered interpretations that would challenge this exclusive association between GAS and ARF. More recent epidemiological observations in ARF endemic regions,^{18,24} clinical reports^{19,25–27} and RAV model data²¹ suggested that SDSE may also be associated with ARF and associated neurobehavioral changes, thereby questioning the hitherto held dogma. Indeed, comparisons of GAS and SDSE genomes clearly suggest that these two species are closely related, and share many virulence genes, including the genes for M proteins.^{20,28–30} Hence, it is conceivable that the disease spectra owing to these two species may overlap.¹⁷ However, thus far lack of an animal model prevented experimental demonstration of association between SDSE infection and ARF.³¹ More importantly, as analogous proteins from these two species trigger the pathological changes, we hypothesize that ARF/RHD pathogenic mechanisms by these two streptococci are similar. In this seminal study we have built on the work carried out by Sikder *et al.*²¹ and demonstrated in a rat model that M proteins from both GAS and SDSE triggered immunological changes and neurobehavioral abnormalities akin to what would be observed in patients having carditis and SC in ARF.^{32–34}

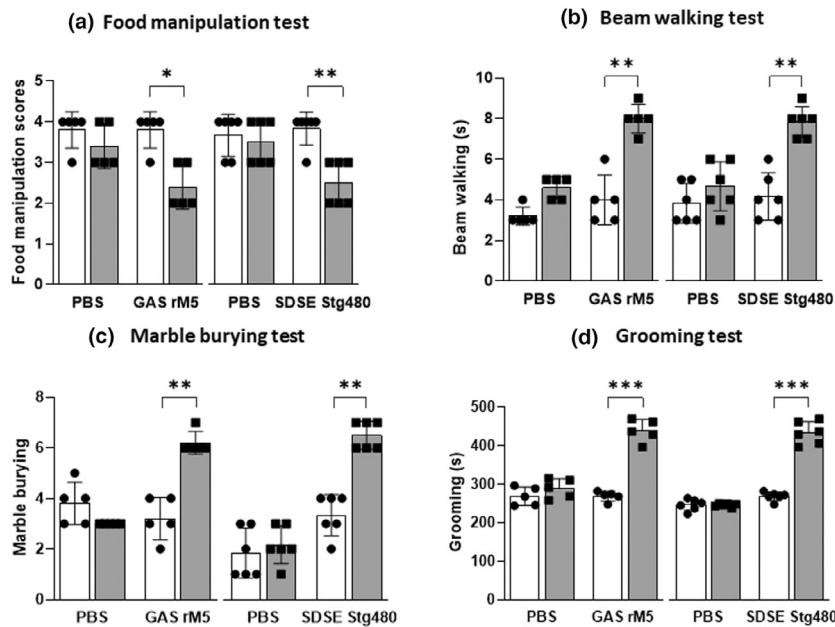


Figure 4. Neurobehavioral abnormalities in rats following exposure to streptococcal recombinant proteins. A series of behavioral experiments including (a) food manipulation, (b) beam walking, (c) marble burying, (d) grooming and (e) light/dark box test (Supplementary figure 2) were performed to assess the neurobehavioral abnormalities (both motor and obsessive-compulsive behavior) in rats before (closed circles) and after (closed squares) injection with streptococcal recombinant proteins. Following injection with streptococcal M proteins, there was impairment in (a) food manipulation and (b) gait and balance compared with controls rats injected with PBS. In addition, rats injected with streptococcal recombinant proteins (c) buried higher number of marbles than control rats and (d) spent more time in induced grooming, compared with controls rats. Data are from one of two experiments with age-matched rats injected with GAS rM5 ($n = 5$) and SDSE Stg480 ($n = 6$). * $P < 0.05$, ** $P < 0.01$, *** $P < 0.001$, by two-way ANOVA with Tukey's *post hoc* multiple comparison test. GAS, group A streptococcus; PBS, phosphate-buffered saline; SDSE, *Streptococcus dysgalactiae* subspecies *equisimilis*.

ARF/RHD and associated neurobehavioral abnormalities result from immune responses initiated by antibodies and T cells that target host cardiac and neuronal proteins.¹ Molecular mimicry or similarity between epitopes of streptococcal antigens and cardiac and neuronal proteins is considered to be one of the mechanisms responsible for the pathogenesis of ARF/RHD.^{1,35–38} Streptococcal M protein shares structural homology with α -helical coiled-coil human proteins such as cardiac myosin,³ tropomyosin,⁴ laminin,⁵ keratin⁶ and vimentin.⁶ In addition, M proteins contain conserved brain-cross-reactive epitopes³⁹ and are involved in the generation of cross-reactive antibodies.^{40,41} These cross-reactive antibodies in ARF are capable of recognizing both extra and intracellular proteins, which can lead to an inflammatory response and untoward cell signaling.^{4,42–44} Anti-streptococcal antibody and interleukin-17A/interferon- γ T-cell responses in the development of carditis are very well documented using animal models^{21,45} and human studies.⁴⁶ Studies investigating these neurobehavioral abnormalities associated with streptococcal infection are in their

infancy.^{21,47} None of the previous animal studies could offer a model for observing concurrent changes in cardiac and neurobehavioral symptoms, following exposure to GAS or SDSE M proteins. The study by Sikder *et al.*²¹ has only demonstrated the cross-reactivity of anti-SDSE antibodies with cardiac myosin. In our current study, we found that anti-streptococcal antibodies cross-reacted with several other α -helical coiled-coil proteins such as cardiac myosin, tropomyosin and laminin. These antibodies also reacted with collagens I and IV, DR1 and DR2, lysoganglioside_{GM1} and tubulin.

Laminin is present in the extracellular matrix of basement membrane of valvular endothelium and it may be the initial target of anti-streptococcal antibodies in ARF/RHD.^{40,48} The molecular recognition of these extracellular proteins by anti-streptococcal antibodies could expose the cryptic epitopes of intracellular proteins such as cardiac myosin, tropomyosin and vimentin. In susceptible individuals, the inflammatory process could further progress through epitope spreading. Furthermore, the cross-reactivity of anti-streptococcal antibodies with intracellular and extracellular proteins lead to cellular

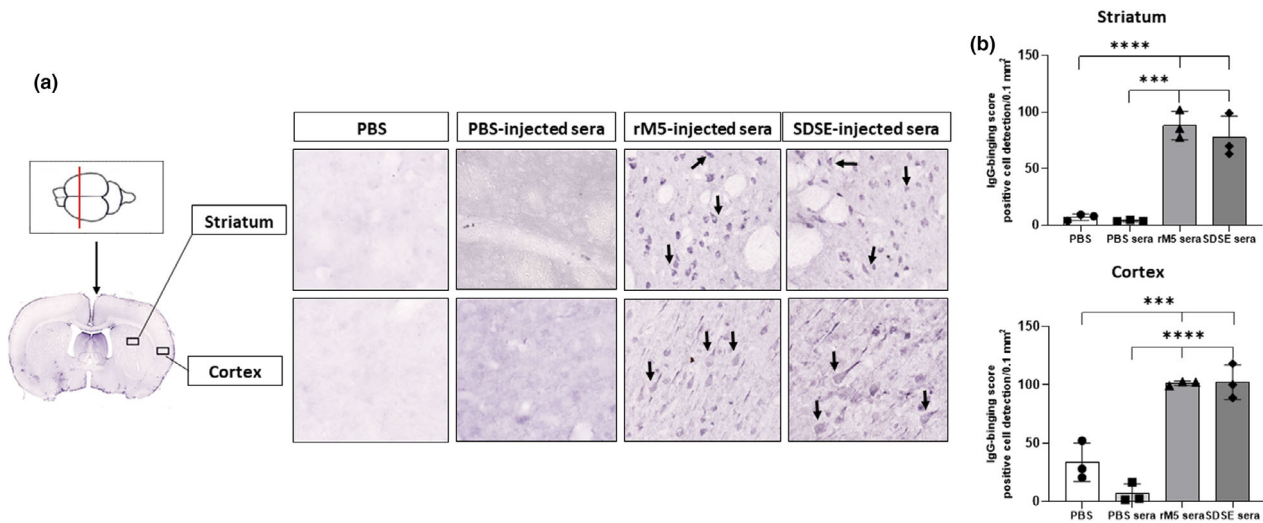


Figure 5. Serum IgG from rats injected with streptococcal recombinant proteins binds to neuronal tissue. Representative images of the striatum and cortex demonstrate binding of serum IgG from rats injected with streptococcal recombinant proteins. Significantly higher serum IgG binding was observed in the striatum and cortex incubated with serum from rats injected with GAS rM5 and SDSE Stg480 than that from rats with PBS. **(a)** Arrows show IgG binding. **(b)** IgG-binding scores were significantly higher in serum from Lewis rats injected with GAS rM5 (closed triangles) and SDSE stg480 (closed diamonds) than from control rats with PBS (closed squares) and PBS (closed circles). Mean number of positive cells in three different sections of the striatum and cortex were detected in 0.1 mm² at 20 \times magnification. Data are from one of the two experiments with age-matched rats injected with GAS rM5 ($n = 5$) and SDSE Stg480 ($n = 6$). *** $P < 0.001$, **** $P < 0.0001$ by one-way ANOVA with Tukey's *post hoc* multiple comparison test. GAS, group A streptococcus; Ig, immunoglobulin; PBS, phosphate-buffered saline; SDSE, *Streptococcus dysgalactiae* subspecies *equisimilis*.

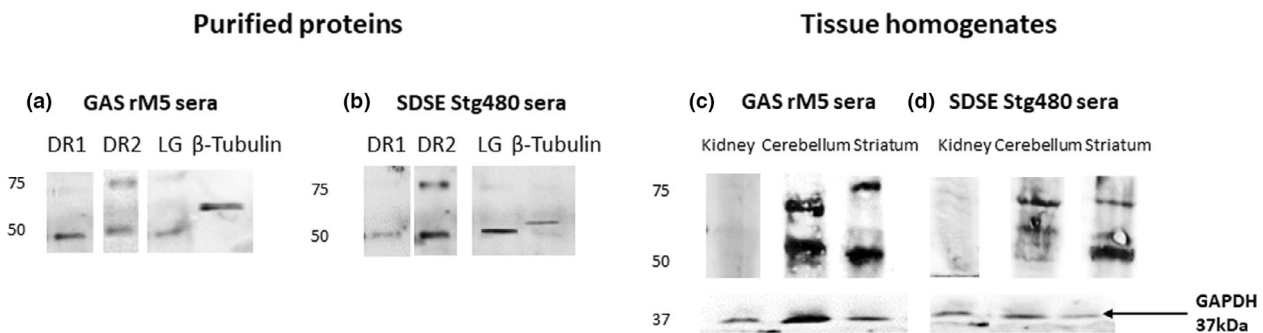


Figure 6. Representative western blot images illustrate the binding pattern of the IgG from pooled sera of rats injected with GAS rM5 **(a)** and SDSE Stg480 **(b)** with purified DR1 and DR2, tubulin and lysoganglioside_{GM1} and bands on these blots were observed at ~48, ~50 and ~52 kDa. Antibodies in pooled sera from rats injected with GAS rM5 **(c)** and SDSE Stg480 **(d)** to lysates of the striatum and cerebellum from naïve rats. Bands on these blots were observed at ~55 and ~70 kDa, which is consistent with the known molecular weights of DR1, DR2, lysoganglioside_{GM1} and tubulin, respectively. Moreover, these sera did not recognize proteins in kidney lysates used as non-neuronal control. Data are from one of two experiments with age-matched rats injected with GAS rM5 ($n = 5$) and SDSE Stg480 ($n = 6$). DR, dopamine receptor; GAS, group A streptococcus; Ig, immunoglobulin; SDSE, *Streptococcus dysgalactiae* subspecies *equisimilis*; GAPDH, Glyceraldehyde-3-phosphate dehydrogenase.

alteration in the valvular endothelium and upregulate expression of cell adhesion molecules and initiate the migration of inflammatory cells into the valve.^{40,43,49}

In addition to cross-reactive antibodies and T cells against GAS M protein, anti-collagen antibodies may also contribute to the disease progression. Elevated levels of

antibodies against collagens I and IV have been observed in ARF.^{7,8,50,51} GAS infection disrupts the extracellular matrix and exposes cryptic collagen epitopes that induce autoantibody response against collagens I and IV.^{52,53} Some GAS M proteins contain a peptide motif (peptide associated with rheumatic fever) essential for the

interaction with collagen IV.^{8,54} However, a recent analysis of GAS isolates associated with ARF revealed that only few of the GAS strains carried the peptide associated with rheumatic fever motif, suggesting that other mechanisms may also contribute to the development of collagen autoantibodies in ARF.⁵⁵ Not only GAS but also SDSE is capable of inducing collagen antibodies through the M-like protein fibrinogen-binding protein (FOG) with amino acid sequence similar to the peptide associated with rheumatic fever motif.⁵⁴ Furthermore, patients with ARF had elevated levels of both collagen autoantibodies and antibodies against FOG, suggesting the contribution of streptococcal species with FOG-positive strains in the pathogenesis of ARF.⁵⁴

Clinical and preclinical studies have demonstrated that carditis is initiated by anti-streptococcal antibodies followed by T-cell infiltration into the valve and myocardium.^{1,21,45,49,56,57} Studies conducted by Dileepan *et al.*⁴⁷ and Platt *et al.*⁵⁸ demonstrated that in the brain, cross-reactive antibodies produced during a GAS infection facilitate a T helper 17 cellular response. Precisely how the inflammatory response and the induction of an interleukin-17A cellular response disrupt the blood–brain barrier to promote anti-streptococcal antibodies to cross this barrier and interact with neuronal proteins remain to be elucidated.

Inflammatory changes that occur in the myocardium and valvular tissue as a result of mononuclear cell infiltration are classical histological features of ARF/RHD.⁴⁹ Carditis is the most common complication in ARF, occurring in more than 50% of patients and is a major Jones criterion for the diagnosis of ARF. The pathological changes in mitral valve and myocardium are characterized by specific lesions known as Aschoff nodules.¹ In the current study, all the rats injected with M proteins of GAS and SDSE showed evidence of carditis with increased infiltration of mononuclear cells including CD3⁺ T lymphocytes and CD68⁺ macrophages into the myocardium and valvular tissues compared with control rats. Similar pathological changes were observed previously in Lewis rats injected with GAS rM6,⁵⁹ peptides from the B- and C-repeat regions of the GAS M5 protein,^{56,60} whole-killed GAS,²¹ GAS rM5⁵⁷ and SDSE or SDSE Stg480.²¹ Prolonged P–R interval in the ECG is a minor Jones criterion that reflects the conduction abnormalities in patients with ARF/RHD.¹ In summary, this and other studies have demonstrated that rats injected with streptococcal antigens develop inflammatory changes leading to conduction abnormalities as reflected by prolonged P–R intervals on ECG.^{21,45,57}

Previous animal studies demonstrated that exposure to GAS is associated with abnormal behavior, and the

adoptive transfer of sera from these GAS-exposed animals to naïve animals can induce these abnormalities in recipient animals.^{61–64} In the current study, rats injected with GAS and SDSE M proteins showed impairment in food manipulation and traversing the narrow beam, a feature of impairment to fine motor control, gait and balance similar to the behavioral abnormalities observed in patients with SC.³⁴ None of the rats injected with streptococcal recombinant proteins and PBS developed anxiety, which further supports that the impairment in traversing a narrow beam is possibly because of abnormalities in gait and balance rather a result of anxiety. Moreover, rats injected with streptococcal recombinant proteins showed increased grooming and marble-burying behaviors compared with PBS controls, suggesting increases in obsessive–compulsive behavior in these rats similar to obsessive–compulsive behavioral defects observed in patients with SC.^{34,65,66} Our results support a causal relationship between exposure to GAS or SDSE M proteins and the development of symptomatology previously demonstrated by Hoffman *et al.*,⁶¹ Brimberg *et al.*⁶³ and Macri *et al.*⁶⁷

Serum from rats injected with GAS rM5 and SDSE Stg480 showed significantly higher serum IgG binding to the striatum and cortex. These antibodies also showed cross-reactivity with neuronal proteins including DR1 and DR2, tubulin and lysoganglioside_{GMI}.⁶⁸ These findings are concordant with earlier studies demonstrating that antibodies from patients with SC strongly react with fragment of type 5 streptococcal M protein (pepM5).³⁹ IgG binding to the striatum may lead to impairment in motor coordination observed in children with SC, whereas IgG binding to the brain striatum and cortex can partially explain behavior observed in obsessive–compulsive disorder. The specific molecular targets on the striatum and cortex were not evaluated in this study.

The tissue targets in ARF/RHD by autoreactive antibodies and T lymphocytes have been partly explored in human and animal studies.^{21,56,57,59,69,70} However, the target antigens of neurobehavioral abnormalities associated with ARF/RHD remain undetermined. Evidence from previous studies^{10,37,68,71} as well as from this study support the hypothesis that DRs, lysoganglioside and tubulin are likely targets. The RAV model can be used to further characterize these targets to determine the sequential development of neurobehavioral abnormalities associated with streptococcal infection. Although an association between streptococcal infection, antineuronal antibodies and neurobehavioral symptomatology is well established, there are many gaps in understanding the pathophysiology of neurobehavioral abnormalities associated with streptococcal infection. It is

unclear how the antibodies generated following streptococcal infections cross the blood–brain barrier and bind to the specific cellular targets to cause antibody-mediated changes in the brain that translate to behavioral abnormalities.

While the pathology of ARF/RHD and associated neurobehavioral abnormalities is multifactorial, we have experimentally demonstrated that antibodies against streptococcal M protein antigens drive the early events, including the generation of antibodies that cross-react with both intracellular and extracellular host cardiac and neuronal proteins. This study validates the use of the RAV model to investigate both cardiac and neurobehavioral sequelae observed in ARF/RHD. Future adoptive transfer studies are necessary to determine how the anti-streptococcal antibodies are able to cross the blood–brain barrier to cause neurobehavioral abnormalities. These studies have far-reaching implications for clinical and community practice. Furthermore, an understanding of the common epitopes of GAS and SDSE M protein that generate cross-reactive antibodies and T cells against host proteins is important to avoid in designing epitope-based vaccine strategies and to identify specific biomarkers of disease and disease progression.

METHODS

Animals

All experimental protocols involving animals were approved by the Animal Ethics Committee of University of New England (AEC 19–013). Female Lewis rats (LEW/SsN; Albino: a,h,c:RT¹), aged 4–8 weeks and weighing between 130 and 200 g, were purchased from the Centre for Animal Research and Teaching, University of New England, Australia. All the rats were acclimatized for 5 days prior to experimentation.

Preparation of GAS and SDSE M proteins

Recombinant M5 protein of GAS (rM5) and SDSE (Stg480) was cloned and purified as described previously.⁵⁶ Briefly, GAS *emm5* and SDSE *stg480* from the NS3396 isolate were cloned into pREP4 and pJ404 vectors, respectively, and expressed in BL21 *E.coli*. In 1-L Luria–Bertani cultures, heterologous protein expression was induced by 1 mM Isopropyl β -D-1-thiogalactopyranoside (IPTG) (Sigma, St Louis, MO, USA) for 24 h. Recombinant M proteins were purified using Ni-NTA resin (Sigma, St Louis, MO, USA) and concentrations of purified proteins were determined using the Bradford assay (Bio-Rad, USA). Lipopolysaccharide contamination in recombinant protein preparations was removed by Triton X-114 (Sigma, St Louis, MO, USA) assisted lipopolysaccharide extraction as previously described.⁷²

Experimental design and injection protocol

In all experiments, baseline behavioral tests and ECG were performed prior to injections. All priming injections were performed under isoflurane inhalation anesthesia (5% induction and 2% maintenance). Six rats per group were subcutaneously injected with 0.5 mg per 100 μ L of recombinant GAS M5 protein or Stg480 antigens emulsified in complete Freund's adjuvant (Sigma, St Louis, MO, USA) in the hock as described previously.⁷³ Control rats were injected with PBS emulsified in complete Freund's adjuvant. On days 1 and 3 all rats were intraperitoneally injected with 0.3 μ g of *Bordetella pertussis* toxin (Thermo Fisher Scientific, Waltham, MA, USA) in 200 μ L PBS. On days 7, 14, 21 and 56, all rats received a booster injection of the respective antigens in incomplete Freund's adjuvants (Sigma, St Louis, MO, USA) on the flank. The rats were killed on day 70 from the day of primary injection with the overdose (260 mg kg⁻¹) of sodium pentobarbital; blood was collected by cardiac puncture, perfused with PBS/10% formalin and heart and brain samples were collected and fixed with 4% paraformaldehyde. Experiments with GAS rM5 were repeated twice ($n = 5$ and 6) with age-matched male and female Lewis rats and experiments with SDSE Stg480 were performed in female rats ($n = 6$).

Detection of serum antibody by ELISA

Serum antibody reactivity against GAS rM5 and SDSE Stg480 and purified host proteins including cardiac myosin, tropomyosin, laminin, collagens I and IV (Sigma, St Louis, MO, USA), DR1 and DR2 (Aviva System Biology, USA), tubulin (MP Biomedicals, USA) and lysoganglioside_{GM1} (Sigma, St Louis, MO, USA) was determined using indirect ELISA. Collagens I and IV were heat denatured at 55–60°C for 5 min to maximize the hydrophobic interaction between collagens I and IV with ELISA plates (Supplementary figure 1).

In brief, 100 μ L of antigens (1 μ g mL⁻¹ of GAS rM5 and SDSE Stg480 and 10 μ g mL⁻¹ of cardiac myosin, tropomyosin, laminin, collagens I and IV, DR1 and DR2, tubulin and lysoganglioside_{GM1}) were coated onto MaxiSorp 96-well plates (Nunc, USA) in carbonate bicarbonate coating buffer (pH 9.6) by incubating the plate at 4°C overnight. Plates were washed three times with wash buffer (PBS/0.02% Tween 20) and blocked with 100 μ L of 1% bovine serum albumin (Thermo Fisher Scientific, Waltham, MA, USA) in wash buffer. Individual rat sera were added in duplicate at 1:400 dilution and incubated at room temperature (20–25°C) for 2 h with agitation. Following repeated washing of the plates, each well was incubated with 100 μ L of goat anti-rat IgG horseradish peroxidase-conjugated secondary antibody (1:5000; Jackson ImmunoResearch, West Grove, PA, USA) for an hour at room temperature. Each well was washed four times with 100 μ L of wash buffer, the plate dried and 100 μ L of 2,2'-azino-di (3-ethylbenzthiazoline)-6-sulfonate (Sigma, St Louis, MO, USA) was added to each well and the plates were incubated for 20 min. Absorbance was measured at 414 nm

using SpectraMax M2/M2e (Molecular Devices, USA). Each serum sample was assessed in duplicate for validation of the results. ELISA plates were normalized with interpolate calibration to reduce the within- and between-plate variability. The coefficient of variability was less than 10% for coating concentration of antigen and concentration of serum.

Electrocardiography

ECG was performed in all rats prior to injection and a day before killing to assess the cardiac dysfunction of rats.²² In brief, rats were anesthetized and ECG traces were recorded for 1–2 min using Bio Amp with the PowerLab data acquisition system (ADInstruments, USA). ECG data were visualized using LabChart 8 software (ADInstruments, USA) and the values of P and R peaks in three different segments of ECG for each rat were individually extracted and analyzed.

Histology and Immunohistochemistry of cardiac tissue

To examine the extent of inflammation, formalin-fixed cardiac tissue was processed, embedded in paraffin, sectioned and stained with Harris hematoxylin and eosin using standard procedures as previously described.⁵⁶ These sections were scored using a validated semiquantitative scoring system.²¹

Formalin-fixed, paraffin-embedded sections (5 μ m) were deparaffinized in xylene and rehydrated with graded ethanol. Epitope retrieval was done with 10 mM Tris-ethylenediaminetetraacetic acid (pH 9.0) for 15 min at 700 W in a laboratory microwave. Sections were incubated in 3% H₂O₂ for 10 min to inhibit endogenous peroxidase activity and rinsed in 10 mM Tris-buffered saline (TBS) at pH 8.4 three times for 5 min. Sections were then blocked with 10% normal sheep serum in TBS for an hour. Blocking buffer was removed and incubated with rat anti-CD3⁺ and rat anti-CD68⁺ (Abcam, USA) at 4°C overnight in a humidified chamber. Sections were washed in TBS and incubated with biotinylated goat anti-rat IgG (Jackson ImmunoResearch, USA) diluted at 1:500 for 2 h at room temperature in a humidified atmosphere. After rinsing in TBS, sections were incubated with avidin–biotin complex (VECTASTAIN Elite ABC-Peroxidase Kit) for an hour at room temperature in a humidified environment. Sections were rinsed thrice in TBS and developed using 3,3'-diaminobenzidine (DAB) substrate (Sigma, St Louis, MO, USA) and counterstained with Harris hematoxylin.

Behavioral assessments

Behavioral tests, including food manipulation, beam walking, grooming, marble burying and light and dark box tests, were performed on rats as previously described.²² In brief, a food manipulation test was carried out to determine the impairment in fine motor control. Food-deprived rats were provided with 2 g of food pellet and assessed for their ability to manipulate the food before and after injection with streptococcal recombinant proteins under infrared light. A

beam walking test was performed to determine abnormalities in gait and balance. Rats were given three trials each in wide (5 cm) and narrow beams (2.5 cm). Following three trials, time taken to transfer the narrow beam was recorded.

Induced grooming tests and marble burying tests were performed to determine the obsessive–compulsive behavior. To initiate induced grooming, rats were sprayed with water and the grooming behavior of the individual animal was recorded over a period of 20 min under infrared light to determine total grooming time. For the marble burying test, rats were placed in a cage at 5-cm depth of corncob bedding with nine marbles in two rows. The number of marbles buried after 10 min were manually counted by a researcher.

Light/dark box tests were performed to determine the anxiety level of rats injected with streptococcal antigens. Rats were placed in the dark compartment of a dual chamber apparatus and were allowed to freely explore both the dark and the brightly lit compartments for 5 min. The time spent by each rat in the light compartment and the number of times rats entered the light compartment were recorded. All sessions were recorded with an HD digital video recorder (Swann, Australia) and assessed blindly; light/dark box data were analyzed using ANY-maze software (Stoelting Co., Wood Dale, IL, USA).

Immunohistochemistry of brain tissue

Binding of serum antibodies from rats injected with GAS rM5 and SDSE Stg480 to brain tissue was assessed by immunohistochemistry using free-floating 40- μ m brain sections from naïve uninjected rats. Brain tissue was dissected from naïve rats following transcardial perfusion with 4% paraformaldehyde in 0.2 M sodium phosphate buffer (PB) and postfixed in 10% formalin overnight at 4°C. Brain sections were washed with 0.1 M PB (pH 7.4), 50% ethanol and 50% ethanol with 3% H₂O₂ for 30 min, respectively, with gentle agitation. Sections were blocked with 2% normal sheep serum in PBST (0.1 M PB supplemented with 0.2% Tween-20) at room temperature and incubated for 48 h with 1:400 dilution of pooled serum from rats injected with GAS rM, SDSE Stg480 and PBS. Sections were washed thrice and incubated overnight with 1:200 dilution of biotinylated secondary anti-rat IgG (Jackson ImmunoResearch, USA) at room temperature with gentle agitation. Following incubation, sections were washed thrice with 0.1 M PB (pH 7.4) for 20 min and incubated with the avidin–biotin complex (VECTASTAIN Elite ABC-Peroxidase Kit) for 2 h at room temperature with gentle agitation. Sections were then washed two times with 0.1 M PB (pH 7.4) and 0.1 M acetate buffer (pH 6.0) for 20 min each and developed using the DAB substrate (Sigma, Australia) solution by incubating for 15 min. After 15 min of incubation in the DAB solution, a DAB solution of glucose oxidase (Sigma, St Louis, MO, USA) was added and the reaction stopped with 0.1 M acetate buffer (pH 6.0). Following three washes in 0.1 M PB, floating sections were transferred to slides, air dried overnight and rehydrated with ethanol, mounted in the DPX mounting medium (Sigma, Australia), coverslipped and stored at 4°C. Slides were scanned using the NanoZoomer 2.0RS (Hamamatsu Photonics, Japan) slide scanner. Three

different sections of the striatum and cortex were randomly selected from each treatment group (PBS, PBS sera, GAS rM5 sera and SDSE Stg480 sera) for analysis of IgG binding. To analyze the binding of IgG, the .jpg images were opened in QuPath (University of Edinburgh, UK). The images were opened as Bright field H-DAB images and the brightness contrast was set to a pixel value of 0.03–0.18. Automated counting was conducted using Optical Density Sum detection with a minimum area of 150 and a maximum area of 1000 pixels. Raw counts were then converted to number of positive cell detection/area for analysis.

Western blot

Western blot was performed to assess the immunoreactivity of sera from rats injected with GAS rM5 and SDSE with purified neuronal proteins and endogenous proteins from brain homogenate.

Tissue from naïve Lewis rats (rats not treated with streptococcal recombinant proteins) including the striatum and cerebellum from brain and kidney (non-neuronal control) were dissected. Tissues were homogenized with cold PBS with 1 mM ethylenediaminetetraacetic acid in bead bug homogenizer (Sigma, St Louis, MO, USA) for 1 min at 3000g. Following homogenization, radioimmunoprecipitation assay buffer and protease inhibitor cocktail were added and centrifuged at 15000g for 15 min at 4°C. An aliquot of each sample was used to determine the protein concentration by Bradford Assay (Bio-Rad, USA). A 20 µg volume of each tissue lysate from the striatum, cerebellum and kidney and purified DR1 and DR2 (Aviva Systems Biology, USA), tubulin (MP Biomedicals, USA) and lysoganglioside_{GM1} (Sigma, St Louis, MO, USA) was separated using 10% nonreducing sodium dodecyl sulfate–polyacrylamide gel electrophoresis. The fractionated proteins were transferred to a polyvinylidene difluoride membrane (Sigma, St Louis, MO, USA) using Trans-Blot Turbo Transfer System (Bio-Rad, USA) using transfer buffer. Following transfer, the polyvinylidene difluoride membrane was blocked with 1% bovine serum albumin in TBS for 1 h. The membrane was washed in TBS containing 0.1% Tween 20 for 2 × 5 min and incubated overnight at 4°C with 5 mL pooled serum (dilution ratio of 1:400) from rats injected with GAS rM5 and SDSE Stg480 using an end over end mixer. The membrane was washed four times with 30 mL of TBS containing 0.1% Tween 20 at room temperature with gentle agitation and incubated with a 1:10 000 horseradish peroxidase–conjugated goat anti-rat IgG secondary antibody (Jackson ImmunoResearch, USA) at room temperature for 1 h. Following incubation, the membrane was washed eight times with 30 mL of TBS containing 0.1% Tween 20 and developed with Clarity Western ECL substrate (Bio-Rad, USA). Excess substrate was blotted from the membrane and a chemiluminescence and a light image were acquired using the ChemiDoc Imaging System (Bio-Rad, USA). Membrane with tissues lysates were stripped using stripping buffer and re-incubated with GAPDH (glyceraldehyde 3-phosphate dehydrogenase) rabbit monoclonal antibody (Cell Signaling Technologies, USA) to

determine the expression of housekeeping proteins and developed with substrate.

Statistical analysis

The behavioral data, ECG, histological scoring and absorbance (optical density values) were assessed using GraphPad Prism 8 (GraphPad, USA). All data from the experimental and control groups passed D'Agostino and Pearson omnibus normality tests. Tests of significance of the behavioral tests and ELISA data were analyzed using one- and two-way ANOVA with Tukey's *post hoc* multiple comparisons test. Nonparametric data were analyzed using the Mann–Whitney *U*-test; *P*-values less than 0.05 were considered significant.

ACKNOWLEDGMENTS

The authors acknowledge Dr Rhonda Davey for the assistance with histology and Dr Daniel Ebert for logistical support and Mr Lachlan Davidson for the assistance with animal experiments. Rukshan AM Rafeek is a recipient of the International Postgraduate Research Award (IPRA) from University of New England. This work was partly supported by an NHMRC Ideas Grant (APP 2010336). Open access publishing facilitated by University of New England, as part of the Wiley - University of New England agreement via the Council of Australian University Librarians.

AUTHOR CONTRIBUTIONS

Rukshan Ahamed Mohamed Rafeek: Conceptualization; data curation; formal analysis; investigation; methodology; resources; validation; writing – original draft; writing – review and editing. **Adam Scott Hamlin:** Data curation; formal analysis; methodology; resources; supervision; validation; writing – review and editing. **Nicholas Matthew Andronicos:** Methodology; resources; supervision; writing – review and editing. **Craig Stephen Lawlor:** Formal analysis; methodology; resources. **David John McMillan:** Conceptualization; formal analysis; funding acquisition; methodology; resources; supervision; writing – review and editing. **Kadaba Srinivasa Sriprakash:** Conceptualization; funding acquisition; methodology; resources; supervision; writing – review and editing. **Natkunam Ketheesan:** Conceptualization; data curation; formal analysis; funding acquisition; methodology; project administration; resources; supervision; writing – review and editing.

CONFLICT OF INTEREST

No conflicts of interest relevant to this manuscript were reported.

REFERENCES

- Carapetis JR, Beaton A, Cunningham MW, *et al.* Acute rheumatic fever and rheumatic heart disease. *Nat Rev Dis Primers* 2016; 2: 15084.

2. Cunningham MW. Autoimmunity and molecular mimicry in the pathogenesis of post-streptococcal heart disease. *Front Biosci* 2003; **8**: s533–s543.
3. Dale J, Beachey E. Epitopes of streptococcal M proteins shared with cardiac myosin. *J Exp Med* 1985; **162**: 583–591.
4. Fenderson PG, Fischetti VA, Cunningham MW. Tropomyosin shares immunologic epitopes with group A streptococcal M proteins. *J Immunol* 1989; **142**: 2475–2481.
5. Vashishtha A, Fischetti VA. Surface-exposed conserved region of the streptococcal M protein induces antibodies cross-reactive with denatured forms of myosin. *J Immunol* 1993; **150**: 4693–4701.
6. Manjula BN, Trus BL, Fischetti VA. Presence of two distinct regions in the coiled-coil structure of the streptococcal Pep M5 protein: relationship to mammalian coiled-coil proteins and implications to its biological properties. *Proc Natl Acad Sci USA* 1985; **82**: 1064–1068.
7. Martins TB, Hoffman JL, Augustine NH, et al. Comprehensive analysis of antibody responses to streptococcal and tissue antigens in patients with acute rheumatic fever. *Int Immunol* 2008; **20**: 445–452.
8. Dinkla K, Talay SR, Morgelin M, et al. Crucial role of the CB3-region of collagen IV in PARF-induced acute rheumatic fever. *PLoS One* 2009; **4**: e4666.
9. Dinkla K, Rohde M, Jansen WT, Kaplan EL, Chhatwal GS, Talay SR. Rheumatic fever-associated *Streptococcus pyogenes* isolates aggregate collagen. *J Clin Invest* 2003; **111**: 1905–1912.
10. Cox CJ, Sharma M, Leckman JF, et al. Brain human monoclonal autoantibody from sydenham chorea targets dopaminergic neurons in transgenic mice and signals dopamine D2 receptor: implications in human disease. *J Immunol* 2013; **191**: 5524–5541.
11. Williams GS. Group C and G streptococci infections: emerging challenges. *Clin Lab Sci* 2003; **16**: 209–213.
12. Sylvestry N, Raveh D, Schlesinger Y, Rudensky B, Yinnon AM. Bacteremia due to beta-hemolytic *Streptococcus* group G: increasing incidence and clinical characteristics of patients. *Am J Med* 2002; **112**: 622–626.
13. Hindsholm M, Schönheyder HC. Clinical presentation and outcome of bacteraemia caused by beta-haemolytic streptococci serogroup G. *APMIS* 2002; **110**: 554–558.
14. Ekelund K, Skinhøj P, Madsen J, Konradsen HB. Invasive group A, B, C and G streptococcal infections in Denmark 1999–2002: epidemiological and clinical aspects. *Clin Microbiol Infect* 2005; **11**: 569–576.
15. Efstratiou A. Pyogenic streptococci of Lancefield groups C and G as pathogens in man. *Soc Appl Bacteriol Symp Ser* 1997; **26**: 72s–79s.
16. Cohen-Poradosu R, Jaffe J, Lavi D, et al. Group G streptococcal bacteremia in Jerusalem. *Emerg Infect Dis* 2004; **10**: 1455–1460.
17. Bramhachari PV, Kaul SY, McMillan DJ, Shaila MS, Karmarkar MG, Sriprakash KS. Disease burden due to *Streptococcus dysgalactiae* subsp. *equisimilis* (group G and C streptococcus) is higher than that due to *Streptococcus pyogenes* among Mumbai school children. *J Med Microbiol* 2010; **59**: 220–223.
18. Haidan A, Talay SR, Rohde M, Sriprakash KS, Currie BJ, Chhatwal GS. Pharyngeal carriage of group C and group G streptococci and acute rheumatic fever in an Aboriginal population. *Lancet* 2000; **356**: 1167–1169.
19. Okumura R, Yamazaki S, Ohashi T, et al. Neuropsychiatric Disorder Associated with Group G *Streptococcus* Infection. *Case Rep Pediatr* 2018; **2018**: 6047318.
20. Davies MR, Tran TN, McMillan DJ, Gardiner DL, Currie BJ, Sriprakash KS. Inter-species genetic movement may blur the epidemiology of streptococcal diseases in endemic regions. *Microbes Infect* 2005; **7**: 1128–1138.
21. Sikder S, Williams NL, Sorenson AE, et al. Group G *Streptococcus* Induces an Autoimmune Carditis Mediated by Interleukin 17A and Interferon γ in the Lewis Rat Model of Rheumatic Heart Disease. *J Infect Dis* 2018; **218**: 324–335.
22. Rafeek RAM, Lobbe CM, Wilkinson EC, et al. Group A streptococcal antigen exposed rat model to investigate neurobehavioral and cardiac complications associated with post-streptococcal autoimmune sequelae. *Animal Model Exp Med* 2021; **4**: 151–161.
23. McMillan DJ, Rafeek RAM, Norton RE, Good MF, Sriprakash KS, Ketheesan N. In Search of the Holy Grail: A Specific Diagnostic Test for Rheumatic Fever. *Front Cardiovasc Med* 2021; **8**.
24. McDonald M, Towers RJ, Andrews RM, Carapetis JR, Currie BJ. Epidemiology of *Streptococcus dysgalactiae* subsp. *equisimilis* in tropical communities, Northern Australia. *Emerg Infect Dis* 2007; **13**: 1694–1700.
25. O'Sullivan L, Moreland NJ, Webb RH, Upton A, Wilson NJ. Acute rheumatic fever after Group A streptococcus pyoderma and Group G streptococcus pharyngitis. *Pediatr Infect Dis J* 2017; **36**: 692–694.
26. Lennon D. A Clear-cut Case of Acute Rheumatic Fever After Group G Streptococcal Pharyngitis in New Zealand. *Pediatr Infect Dis J* 2018; **37**: 376–377.
27. Chandnani HK, Jain R, Patamasucon P. Group C *Streptococcus* Causing Rheumatic Heart Disease in a Child. *J Emerg Med* 2015; **49**: 12–14.
28. Davies MR, McMillan DJ, Beiko RG, et al. Virulence profiling of *Streptococcus dysgalactiae* Subspecies *equisimilis* isolated from infected humans reveals 2 distinct genetic lineages that do not segregate with their phenotypes or propensity to cause diseases. *Clin Infect Dis* 2007; **44**: 1442–1454.
29. Collins CM, Kimura A, Bisno AL. Group G streptococcal M protein exhibits structural features analogous to those of class I M protein of group A streptococci. *Infect Immun* 1992; **60**: 3689–3696.
30. Jones KF, Fischetti VA. Biological and immunochemical identity of M protein on group G streptococci with M protein on group A streptococci. *Infect Immun* 1987; **55**: 502–506.
31. Rafeek RAM, Sikder S, Hamlin AS, et al. Requirements for a robust animal model to investigate the disease mechanism of autoimmune complications associated with ARF/RHD. *Front Cardiovasc Med* 2021; **8**: 675339.

32. Kaplan MH, Bolande R, Rakita L, Blair J. Presence of bound immunoglobulins and complement in the myocardium in acute rheumatic fever: association with cardiac failure. *N Engl J Med* 1964; **271**: 637–645.
33. Taranta A, Stollerman GH. The relationship of Sydenham's chorea to infection with group A streptococci. *Am J Med* 1956; **20**: 170–175.
34. Gordon N. Sydenham's chorea, and its complications affecting the nervous system. *Brain Dev* 2009; **31**: 11–14.
35. Guilherme L, Kalil J, Cunningham M. Molecular mimicry in the autoimmune pathogenesis of rheumatic heart disease. *Autoimmunity* 2006; **39**: 31–39.
36. Dale RC, Merheb V, Pillai S, *et al.* Antibodies to surface dopamine-2 receptor in autoimmune movement and psychiatric disorders. *Brain* 2012; **135**: 3453–3468.
37. Ben-Pazi H, Stoner JA, Cunningham MW. Dopamine receptor autoantibodies correlate with symptoms in Sydenham's chorea. *PLoS One* 2013; **8**: e73516.
38. Kirvan CA, Cox CJ, Swedo SE, Cunningham MW. Tubulin is a neuronal target of autoantibodies in Sydenham's Chorea. *J Immunol* 2007; **178**: 7412–7421.
39. Bronze MS, Dale JB. Epitopes of streptococcal M proteins that evoke antibodies that cross-react with human brain. *J Immunol* 1993; **151**: 2820–2828.
40. Galvin JE, Hemric ME, Ward K, Cunningham MW. Cytotoxic mAb from rheumatic carditis recognizes heart valves and laminin. *J Clin Invest* 2000; **106**: 217–224.
41. Cunningham MW. Pathogenesis of group A streptococcal infections. *Clin Microbiol Rev* 2000; **13**: 470–511.
42. Cunningham MW, McCormack JM, Fenderson PG, Ho MK, Beachey EH, Dale JB. Human and murine antibodies cross-reactive with streptococcal M protein and myosin recognize the sequence GLN-LYS-SER-LYS-GLN in M protein. *J Immunol* 1989; **143**: 2677–2683.
43. Cunningham MW, Antone SM, Gulizia JM, McManus BM, Fischetti VA, Gauntt CJ. Cytotoxic and viral neutralizing antibodies crossreact with streptococcal M protein, enteroviruses, and human cardiac myosin. *Proc Natl Acad Sci USA* 1992; **89**: 1320–1324.
44. Krisher K, Cunningham MW. Myosin: a link between streptococci and heart. *Science* 1985; **227**: 413–415.
45. Sikder S, Price G, Alim MA, *et al.* Group A streptococcal M-protein specific antibodies and T-cells drive the pathology observed in the rat autoimmune valvulitis model. *Autoimmunity* 2019; **52**: 78–87.
46. Wen Y, Zeng Z, Gui C, Li L, Li W. Changes in the expression of Th17 cell-associated cytokines in the development of rheumatic heart disease. *Cardiovasc Pathol* 2015; **24**: 382–387.
47. Dileepan T, Smith ED, Knowland D, *et al.* Group A Streptococcus intranasal infection promotes CNS infiltration by streptococcal-specific Th17 cells. *J Clin Invest* 2016; **126**: 303–317.
48. Root-Bernstein R. Rethinking Molecular Mimicry in Rheumatic Heart Disease and Autoimmune Myocarditis: Laminin, Collagen IV, CAR, and B1AR as Initial Targets of Disease. *Front Pediatr* 2014; **2**.
49. Roberts S, Kosanke S, Terrence Dunn S, Jankelow D, Duran CM, Cunningham MW. Pathogenic mechanisms in rheumatic carditis: focus on valvular endothelium. *J Infect Dis* 2001; **183**: 507–511.
50. McGregor R, Tay ML, Carlton LH, *et al.* Mapping autoantibodies in children with acute rheumatic fever. *Front Immunol* 2021; **12**.
51. Pilapitiya DH, Harris PWR, Hanson-Manful P, *et al.* Antibody responses to collagen peptides and streptococcal collagen-like 1 proteins in acute rheumatic fever patients. *Pathog Dis* 2021; **79**.
52. Tandon R, Sharma M, Chandrashekar Y, Kotb M, Yacoub MH, Narula J. Revisiting the pathogenesis of rheumatic fever and carditis. *Nat Rev Cardiol* 2013; **10**: 171–177.
53. Karthikeyan G, Guilherme L. Acute rheumatic fever. *Lancet* 2018; **392**: 161–174.
54. Dinkla K, Nitsche-Schmitz DP, Barroso V, *et al.* Identification of a streptococcal octapeptide motif involved in acute rheumatic fever. *J Biol Chem* 2007; **282**: 18686–18693.
55. de Crombrugge G, Baroux N, Botteaux A, *et al.* The limitations of the rheumatogenic concept for Group A streptococcus: systematic review and genetic analysis. *Clin Infect Dis* 2020; **70**: 1453–1460.
56. Gorton D, Govan B, Olive C, Ketheesan N. B- and T-cell responses in group A streptococcus M-protein- or Peptide-induced experimental carditis. *Infect Immun* 2009; **77**: 2177–2183.
57. Gorton D, Sikder S, Williams NL, *et al.* Repeat exposure to group A streptococcal M protein exacerbates cardiac damage in a rat model of rheumatic heart disease. *Autoimmunity* 2016; **49**: 563–570.
58. Platt MP, Bolding KA, Wayne CR, *et al.* Th17 lymphocytes drive vascular and neuronal deficits in a mouse model of postinfectious autoimmune encephalitis. *Proc Natl Acad Sci USA* 2020; **117**: 6708–6716.
59. Quinn A, Kosanke S, Fischetti VA, Factor SM, Cunningham MW. Induction of autoimmune valvular heart disease by recombinant streptococcal m protein. *Infect Immun* 2001; **69**: 4072–4078.
60. Lymbury RS, Olive C, Powell KA, *et al.* Induction of autoimmune valvulitis in Lewis rats following immunization with peptides from the conserved region of group A streptococcal M protein. *J Autoimmun* 2003; **20**: 211–217.
61. Hoffman KL, Hornig M, Yaddanapudi K, Jabado O, Lipkin WI. A murine model for neuropsychiatric disorders associated with Group A β -hemolytic streptococcal infection. *J Neurosci* 2004; **24**: 1780–1791.
62. Yaddanapudi K, Hornig M, Serge R, *et al.* Passive transfer of streptococcus-induced antibodies reproduces behavioral disturbances in a mouse model of pediatric autoimmune neuropsychiatric disorders associated with streptococcal infection. *Mol Psychiatry* 2010; **15**: 712–726.
63. Brimberg L, Benhar I, Mascaro-Blanco A, *et al.* Behavioral, pharmacological, and immunological abnormalities after streptococcal exposure: a novel rat model of Sydenham chorea and related neuropsychiatric disorders. *Neuropsychopharmacology* 2012; **37**: 2076–2087.

64. Lotan D, Benhar I, Alvarez K, *et al.* Behavioral and neural effects of intra-striatal infusion of anti-streptococcal antibodies in rats. *Brain Behav Immun* 2014; **38**: 249–262.
65. Swedo SE, Rapoport JL, Cheslow DL, *et al.* High prevalence of obsessive-compulsive symptoms in patients with Sydenham's chorea. *Am J Psychiatry* 1989; **146**: 246–249.
66. Pudukollu M, Mushet N, Linney M, Hennessy C, Morton M. Neuropsychiatric manifestations of Sydenham's chorea: a systematic review. *Dev Med Child Neurol* 2016; **58**: 16–28.
67. Macri S, Ceci C, Onori MP, *et al.* Mice repeatedly exposed to Group-A β -Haemolytic Streptococcus show perseverative behaviors, impaired sensorimotor gating, and immune activation in rostral diencephalon. *Sci Rep* 2015; **5**: 13257.
68. Chain JL, Alvarez K, Mascaro-Blanco A, *et al.* Autoantibody biomarkers for basal ganglia encephalitis in sydenham chorea and pediatric autoimmune neuropsychiatric disorder associated with streptococcal infections. *Front Psych* 2020; **11**: 564.
69. Kirvan CA, Galvin JE, Hilt S, Kosanke S, Cunningham MW. Identification of streptococcal m-protein cardiopathogenic epitopes in experimental autoimmune valvulitis. *J Cardiovasc Transl Res* 2014; **7**: 172–181.
70. Ellis NM, Li Y, Hildebrand W, Fischetti VA, Cunningham MW. T cell mimicry and epitope specificity of cross-reactive T cell clones from rheumatic heart disease. *J Immunol* 2005; **175**: 5448–5456.
71. Singer HS, Mascaro-Blanco A, Alvarez K, *et al.* Neuronal antibody biomarkers for Sydenham's chorea identify a new group of children with chronic recurrent episodic acute exacerbations of tic and obsessive compulsive symptoms following a streptococcal infection. *PLoS One* 2015; **10**: e0120499.
72. Teodorowicz M, Perdijk O, Verhoek I, *et al.* Optimized Triton X-114 assisted lipopolysaccharide (LPS) removal method reveals the immunomodulatory effect of food proteins. *PLoS One* 2017; **12**: e0173778.
73. Gorton D, Blyth S, Gorton JG, Govan B, Ketheesan N. An alternative technique for the induction of autoimmune valvulitis in a rat model of rheumatic heart disease. *J Immunol Methods* 2010; **355**: 80–85.

SUPPORTING INFORMATION

Additional supporting information may be found online in the Supporting Information section at the end of the article.

© 2022 The Authors. *Immunology & Cell Biology* published by John Wiley & Sons Australia, Ltd on behalf of Australian and New Zealand Society for Immunology, Inc.

This is an open access article under the terms of the Creative Commons Attribution-NonCommercial-NoDerivs License, which permits use and distribution in any medium, provided the original work is properly cited, the use is non-commercial and no modifications or adaptations are made.